

# Maximum spoutable bed height of spout-fluid bed

Wenqi Zhong\*, Mingyao Zhang, Baosheng Jin

*Key Laboratory on Clean Coal Power Generation and Combustion Technology of Ministry of Education,  
Thermoenergy Engineering Research Institute, Southeast University, Nanjing 210096, PR China*

Received 18 April 2006; received in revised form 14 August 2006; accepted 17 August 2006

## Abstract

Experimental study on the maximum spoutable bed height of a spout-fluid bed (cross-section of 0.3 m × 0.03 m and height of 2 m) packed with Geldart group D particles has been carried out. The effects of particle size, spout nozzle size and fluidizing gas flow rate on the maximum spoutable bed height were studied. Experimental data were compared to some published experiments and predictions. The results show that the maximum spoutable bed height of spout-fluid bed decreases with increasing particle size and spout nozzle size, which appears the same trend to that of spouted beds. The increasing of fluidizing gas flow rate leads to a sharply decrease in the maximum spoutable bed height. The existent correlations of the maximum spoutable bed height in the literature were observed to involve large discrepancies. Additionally, the flow characteristics when bed materials deeper than the maximum spoutable height were summarized. Under this condition, the spout-fluid bed operated without a stable and coherent spout or fountain assembles the characteristics of jetting fluidized bed. Besides, the mechanisms of spout termination were investigated. It was found that slugging in the spout and growth of instabilities would cause the spout termination in spout-fluid bed.

© 2006 Elsevier B.V. All rights reserved.

*Keywords:* Gas–solid flow; Maximum spoutable bed height; Spout-fluid bed; Spouted bed; Jetting fluidized bed

## 1. Introduction

Spout-fluid bed is one of the modifications of conventional spouted bed, to reduce some of the limitations of spouted bed by introducing fluidizing gas through a porous or perforated distributor surrounding the central nozzle. The fluidizing gas increases the fluid–solid contact in the annular regions and reduces the likelihood of particle agglomeration, dead zones and sticking to the wall of the vessel [1,2].

Recognized as a versatile gas–solid reactor, spout-fluid beds have been of increasing interest in the petrochemical, chemical and metallurgic industries. Many valuable experimental and theoretical studies (e.g. [1–23]) have been carried out in the past twenties years. For example, the group at University of British Columbia (UBC) of Canada have had a very significant role in the effort to understand and apply spout-fluid beds (e.g. [1,2,5,7,11,12]); in Southeast University (SEU) of China, studies on the complex hydrodynamic characteristics and chemical reactions in spout-fluid beds are being performed (e.g. [13–23]),

in order to develop the spout-fluid beds for various applications such as desulfurization, CO<sub>2</sub> capture, combustion and gasification of coal and biomass. However, the spout-fluid bed technique has difficulty in being applied in larger-scale industrial process now due to some limitations, one of which is the lack of full knowledge on the hydrodynamic characteristics.

The maximum spoutable bed height is an important characteristic in the design, operating and scale-up of both spouted beds and spout-fluid beds, because it is directly related to the amount of materials that can be processed, beyond which the spout terminates [24]. However, there has been little published information [6,8] concerning such a characteristic of spout-fluid beds so far, many investigations [25–39] paid attention to spouted beds. The maximum spoutable bed height of spout-fluid is still not completely unveiled. For example, what is the character of the maximum spoutable bed height of spout-fluid bed? Is it similar to a conventional spouted bed? How the fluidizing gas influences the maximum spoutable bed height of spout-fluid bed? What is the gas–solid flow behaviors if the bed material larger than maximum spoutable bed height? Moreover, what the mechanism of spout termination in spout-fluid bed would be? In order to answer these interesting questions, experimental as well as theoretical approaches are needed.

\* Corresponding author. Tel.: +86 25 83795119; fax: +86 25 83795508.  
E-mail address: wqzhong@seu.edu.cn (W. Zhong).

### Nomenclature

$A$	dimensionless parameters in Ref. [32], $A = Re_{mf} Re_t d_p / Ar D_i$
$Ar$	Archimedes number
$d_p$	particle diameter (m)
$D_i$	spout nozzle diameter or width (m)
$D_t$	bed diameter or width (m)
$f$	sampling frequency (Hz)
$h$	ratio of maximum spoutable bed height with fluidizing gas to without fluidizing gas
$H$	bed height (m)
$H_m$	maximum spoutable bed height (m)
$H_0$	static bed height (m)
$Q_f$	fluidizing gas flow rate ( $m^3/s$ )
$Q_{mf}$	minimum fluidizing gas flow rate ( $m^3/s$ )
$Q_s$	spouting gas flow rate ( $m^3/s$ )
$t$	pressure time series sampling time (s)
$u_{mf}$	minimum fluidizing gas velocity (m/s)
$u_t$	particle terminal velocity (m/s)

### Greek letters

$\Delta t$	time interval between successive frames (s)
$\delta$	relative deviation of particle diameter (%)
$\varepsilon$	particles bulk voidage
$\theta$	angle of column base ( $^\circ$ )
$\rho_g$	gas density ( $kg/m^3$ )
$\rho_p$	particle density ( $kg/m^3$ )

In the present work, experiments were carried out on the maximum spoutable bed height in a rectangular spout-fluid bed. It mainly focused on discussing the above-mentioned questions.

## 2. Experiments

### 2.1. Experimental system

The spout-fluid bed experimental system is schematically shown in Fig. 1. This system consists of a spout-fluid bed column, a gas supply system and some sampling instruments. The column has a cross-section of 300 mm  $\times$  30 mm and a height of 2000 mm. It was made of 8 mm thick Plexiglas. The area of the spout nozzle is 30 mm  $\times$  30 mm (the slot width can be adjusted). A conical gas distributor with a 60° inclination angle is located at the bottom of the bed. The orifices in the air distributor are 1 mm in diameter, and the total area of all orifices is 1.1% of the gas distributor.

A Roots-type blower supplied the spouting gas and the fluidizing gas. A pressure-reducing valve was installed to avoid pressure oscillations and achieve a steady gas flow. The gas flow rates were measured by two flow meters. The spouting gas entered the bed directly through the spout nozzle. The fluidizing gas was divided into two equal fluxes by a flux distributor before flowing into the gas chamber, and then entered the bed via the orifices in the gas distributor.

Pressure fluctuations in the bed were obtained by a multi-channel differential pressure signal sampling system. There were fifteen pressure-measuring holes located on the back wall of the column, some in the spout and some in the annular dense regions,

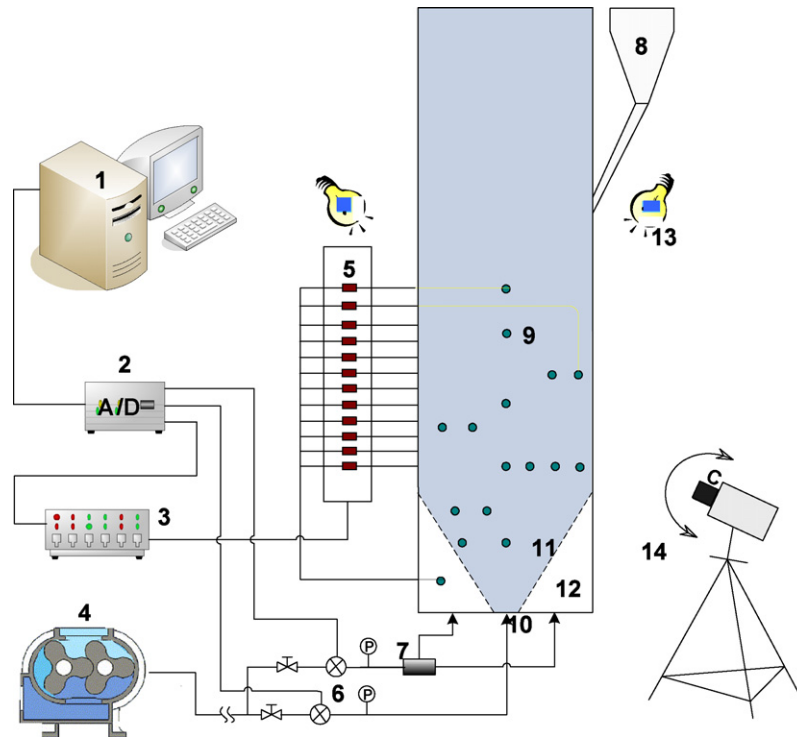


Fig. 1. Schematic diagram of spout-fluid bed experimental system. (1) Computer; (2) A/D converter; (3) multi-channel differential pressure signal transmitter; (4) roots-type blower; (5) differential pressure sensor; (6) flow meter; (7) fluidization flux distributor; (8) material adding tank; (9) pressure port; (10) spout nozzle; (11) gas distributor; (12) fluidizing gas chamber; (13) floodlight; (14) digital CCD.

Table 1  
Experimental and sampling conditions

$H_0$ (mm)	300–550
$Q_s$ (m <sup>3</sup> /s)	0–0.08
$Q_f$ (m <sup>3</sup> /s)	0–0.04
$f$ (Hz)	100
$t$ (s)	180

at heights of 160, 245, 400, 600, 700, and 800 and 1000 mm above the bottom of the bed. Every differential pressure sensor has two ports, one was connected to the pressure-measuring hole in the column wall, and the other was connected to a fluidizing gas chamber. The differential pressures were measured and then converted into voltage signals by multi-channel differential pressure signal transmitter with a scale of 0–16 kPa. The voltage signals were sent to a computer through an A/D converter. A digital camera (Nikon 5000) and a digital video recorder (Sony DCR-PC330E) were employed to photograph the flow regimes through the transparent wall during the experiments. Two groups of 2000 W floodlights were used to enhance the photo definition when photographing.

## 2.2. Operating conditions

Experimental and sampling conditions and particle properties studied in the present work are summarized in Tables 1 and 2, respectively.

## 2.3. Determination of $H_m$

In spouted beds, the maximum bed  $H_m$  was determined by adding amounts of particles stepwise until stable spouting could not be achieved for any spouting gas velocity, which was also be called spout termination [24]. However, spouting in spout-fluid beds is somewhat different from that in spouted beds. Very stable and coherent spouting is difficult to achieve due to the larger porosity in the annular region and large bubbles in the bed surface by introducing the fluidizing gas. Spouting in the spout-fluid bed is periodic and incoherent [16]. Similar to Dogan et al. [36,38] and Freitas et al. [37], in our previous publication [19,20] and present work, we did not consider the periodic and incoherent spouting to be the spout termination, but rather a mode of spouting.  $H_m$  was determined by adding amounts of particles stepwise until periodic and incoherent spouting could not be achieved for any spouting gas velocity at certain fluidizing gas flow rate.

Table 2  
Particle properties

Particles	$d_p$ (mm)	$\delta$ (%)	$\rho_s$ (kg/m <sup>3</sup> )	$\varepsilon$	$u_{mf}$ (m/s)
Mung beans	3.2	10.3	1640	0.42	1.07
Polystyrene beads	2.8	12.1	1018	0.41	0.82
Millet	1.6	8.4	1330	0.40	0.58
Glass beads A	1.3	5.2	2600	0.38	0.62
Glass beads B	1.8	5.2	2600	0.39	1.13
Glass beads C	2.3	5.2	2600	0.40	1.48

## 3. Results and discussion

### 3.1. Experimental data of $H_m$

#### 3.1.1. Effect of particle size

The maximum spoutable bed height  $H_m$  with respect to particle size has been reported by several investigations. Mathur and Epstein [24] indicated that  $H_m$  increases with particle size  $d_p$  up to a limit and then decreases, the critical particle size commonly ranges from 1.0 to 1.5 mm for the columns in different diameters. This tendency was demonstrated by later studies [25–27]. In another study, Rovero et al. [28] indicated that  $H_m$  increased when the particle diameter was increased from 0.3 to 0.45 mm in an 80 mm diameter flat-based column, and then  $H_m$  decreased when the particle diameter was increased from 0.65 to 1.24 mm. The results of Chandnani and Epstein [30] showed that  $H_m$  increased as the particles size was increased from 0.40 to 0.71 mm, and then decreased. These studies on spouted beds showed that  $H_m$  of spouted beds decreases with increasing particle size for coarse particles. This trend of the maximum spoutable bed height respect to particle size can also be seen in the previous reports by Grbavcic et al. [8], Cecen [31], Dogan et al. [36] and Freitas et al. [37].

The effect of particle size on the maximum spoutable bed height  $H_m$  of present spout-fluid bed and some spouted beds in the literature are presented in Fig. 2. The density of particles in Fig. 2 is in the range of 2400–2600 kg/m<sup>3</sup>. The data were obtained in the columns with different geometries, thus the dimensionless parameters  $H_m/D_t$  and  $d_p/D_t$  were used, where,  $D_t$  is the diameter of cylindrical column or the width of rectangular column. The present experimental data show that the effect of particle size on  $H_m$  of spout-fluid bed decreases with increasing  $d_p$ , which displays the same tendency to those of spouted beds.

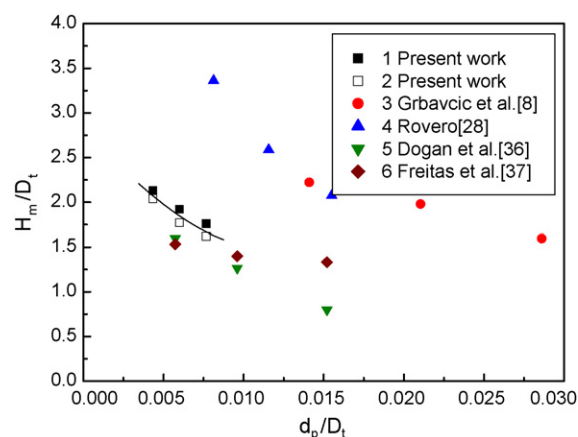


Fig. 2. Effect of particle size on the maximum spoutable bed heights of present spout-fluid bed and some spouted beds in the literature: (1) spout-fluid bed,  $D_i = 20$  mm,  $D_t = 300$  mm, 60° cone base,  $u_f/u_{mf} = 0$ ; (2) spout-fluid bed,  $D_i = 20$  mm,  $D_t = 300$  mm, 60° cone base,  $u_f/u_{mf} = 0.69$ ; (3) half cylindrical spout-fluid bed,  $D_i = 25$  mm,  $D_t = 144$  mm, flat base,  $u_f/u_{mf} = 0$ ; (4) cylindrical spouted bed,  $D_i = 6$  mm,  $D_t = 80$  mm, 40° cone base; (5) rectangular spouted bed,  $D_i = 20$  mm,  $D_t = 150$  mm, 60° cone base; (6) rectangular spouted bed,  $D_i = 2$  mm,  $D_t = 150$  mm, 60° cone base.

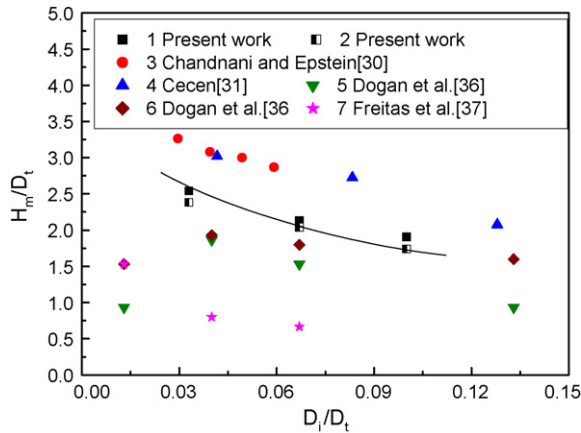


Fig. 3. Effect of spout nozzle size on the maximum spoutable bed heights of present spout-fluid bed and some spouted beds in the literature: (1) spout-fluid bed,  $d_p = 1.3$  mm,  $D_t = 300$  mm,  $60^\circ$  cone base,  $u_f/u_{mf} = 0$ ; (2) spout-fluid bed,  $d_p = 1.3$  mm,  $D_t = 300$  mm,  $60^\circ$  cone base,  $u_f/u_{mf} = 0.69$ ; (3) cylindrical spouted bed,  $d_p = 0.40$  mm,  $D_t = 152$  mm,  $60^\circ$  cone base; (4) half cylindrical spouted bed,  $d_p = 0.65$ – $1.3$  mm,  $D_t = 152.4$  mm, flat base; (5) rectangular spouted bed,  $d_p = 0.86$  mm,  $D_t = 150$  mm,  $60^\circ$  cone base; (6) rectangular spouted bed,  $d_p = 1.44$  mm,  $D_t = 150$  mm,  $60^\circ$  cone base; (7) rectangular spouted bed,  $d_p = 0.86$  mm,  $D_t = 150$  mm,  $60^\circ$  cone base.

### 3.1.2. Effect of spout nozzle size

Fig. 3 shows the effect of spout nozzle size on the maximum spoutable bed heights of present spout-fluid bed and some spouted beds in the literature. It can be seen that  $H_m$  of spout-fluid bed decreases with increasing spout nozzle diameter without reference to the introduction of fluidizing gas.

In the literature, Littman et al. [26] specially studied the effect of spout nozzle diameter on  $H_m$  and demonstrated that  $H_m$  decreased with increasing spout nozzle diameter. Same tendency has been observed by later investigations (e.g. [30,31,37]). Dogan et al. [36] indicated that  $H_m$  increased from the 2 mm spout nozzle width ( $D_i/D_t = 0.013$ ) to the 6 mm spout nozzle width ( $D_i/D_t = 0.04$ ) and then decreases with spout nozzle width, as presented in Fig. 3. Nevertheless, Dogan et al. [38] in their later publication showed that  $H_m$  increased slightly with increasing spout nozzle size. According to the above review, we can draw a generally conclusion that  $H_m$  of spouted beds might decrease with increasing spout nozzle size. In this sense, it is found that the effect of spout nozzle size on  $H_m$  of spout-fluid bed shares the same tendency to those of spouted beds.

### 3.1.3. Effect of fluidizing gas flow rate

There has been little investigation [6,8] on the maximum spoutable height  $H_m$  of a spout-fluid bed, especially the discussion on the effect of fluidizing gas flow rate on  $H_m$  so far. Rao et al. [6] theoretically studied  $H_m$  of a spout-fluid bed under the condition that normal spouting was accompanied by additional aeration but no fluidization of the annulus. Their experiments showed that  $H_m$  decreases with increasing fluidizing gas flow rate. Grbavcic et al. [8] studied  $H_m$  of a flat base spout-fluid bed at minimum spout-fluidizing flow rate and obtained the same results. These studies were carried out at a narrow range of fluidizing gas flow rate (less than minimum fluidizing gas flow rate). However, previous work [17,19,20] illustrated that spouting and

spout-fluidizing could also be observed when the fluidizing gas flow rate is larger than the minimum fluidization condition.

Fig. 3 presents the effect of fluidizing gas flow rate on the maximum spoutable bed height under different bed geometries and operating conditions. In which,  $h$  is the ratio of maximum spoutable bed height with fluidizing gas to without fluidizing gas. It can be seen that the maximum spoutable bed height decreases with fluidizing gas flow rate. This appears a similar tendency to the previous work by Rao et al. [6] for  $60^\circ$  cone base half column and Grbavcic et al. [8] for flat base full column. This result indicates that the spoutable bed height decreases with fluidizing gas flow rate without reference to bed geometry and operating condition.

### 3.2. Verification of existent $H_m$ correlations

The prediction of the maximum spoutable height  $H_m$  is important for successful reactor design. Some correlations of  $H_m$  have been proposed in the literature. They are listed in Table 3.

A comparison of our present experimental results with the prediction calculated by these correlations is shown in Fig. 4. The results show that the present predictions are not in satisfied agreement with the present experimental results. The correlation of Littman et al. [26] overestimates of the  $H_m$  with a deviation between 50% and 75%, while the correlations of Passos et al. [32] and Dogan et al. [38] underestimates of the  $H_m$  with a deviation between 25% and 60%. Most of the predictions calculated by the correlations of McNab and Bridgwater [27] and Cecen [31] are in agreement with the present experimental data with a deviation within 25%, but some of the predictions have relatively large deviation that is in the range of 25–50%.

The deviations might attribute to the following reasons. The predictions fall outside the range where the correlations are said to be valid. Besides, these correlations did not involve the effect of fluidizing gas flow rate, which might lead to errors. As illustrated in Fig. 5, the fluidizing gas takes great effect on  $H_m$ . Rao et al. [6] and Grbavcic et al. [8] developed the correlations to modify the effect of fluidizing gas flow rate on  $H_m$ , while the

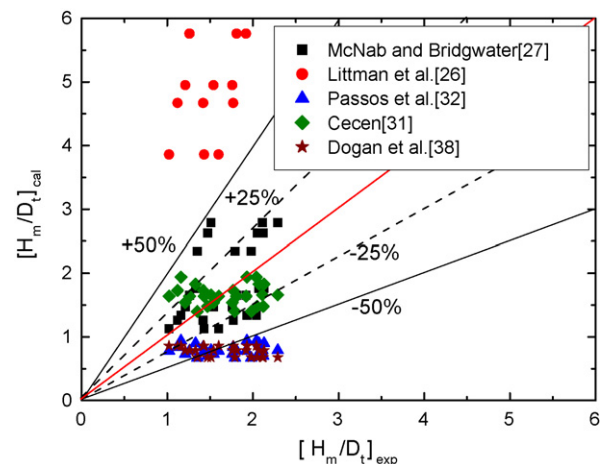


Fig. 4. Comparison of present experimental results with the prediction calculated by the correlations of  $H_m$  in the literature.



Table 3  
Correlations of  $H_m$  in the literature

Author	Correlation
McNab and Bridgewater [27]	$\frac{H_m}{D_t} = \frac{D_t}{d_p} \left( \frac{D_t}{D_i} \right)^{2/3} \frac{700}{Ar} \left( \sqrt{1 + 35.9 \times 10^{-6} Ar} - 1 \right)^2$
Littman et al. [26]	$\frac{H_m}{D_t} = \frac{D_t}{D_i} \left[ 0.218 + 0.005 \left( \frac{\rho_p - \rho_g}{\rho_g} \frac{g D_i}{u_{mf} u_{t1}} \right) \right]$
Passos et al. [32]	$\frac{H_m}{D_t} = 0.605 + \frac{6.21 \times 10^{-2}}{A} - \frac{2.9 \times 10^{-3}}{A^2}$
Cecen [31]	$\frac{H_m}{D_t} = 0.99 \left( \frac{\rho_p - \rho_g}{\rho_g} \frac{g D_i}{u_{mf} u_{t1}} \right)$
Dogan et al. [39]	$\frac{H_m}{D_t} = 1.5 \frac{D_i^{0.21}}{D_t} \theta^{-0.25}$

predictions still involve large discrepancies. As a result, these correlations cannot be used to predict  $H_m$  of the present spout-fluid bed.

The above discussion indicates that particle size, spout nozzle diameter and fluidizing gas flow rate take effect on the maximum spoutable bed height of spout-fluid beds. Besides, parameters as bed density, angle of the contactor base, the ratio between inlet diameter and particle diameter, configuration of the fluidizing gas distributor should be considered in the development of a correlation. Moreover, for the spout-fluid bed gasification, the effects of pressure and tempura on the maximum spoutable bed height should also be considered. However, the present work is not able to perform this valuable step since experiments cover larger range of bed geometry and operating condition are needed.

### 3.3. Flow behaviors when bed materials beyond $H_m$

Spout-fluid beds can be developed for various applications. Generally, the bed height is controlled within the maximum spoutable bed height  $H_m$  in order to form stable spouts for drying, combustion, tablet coating and etc. Besides, spout-fluid beds are also operated at the bed height larger than  $H_m$  for special interest, for example coal gasification [22,23,40].

Coal gasification in the spout-fluid bed is similar to the U-gas or Westinghouse processes. In addition to injecting a part of gasification agent through the central nozzle, gasification agent

is also introduced through a porous or perforated distributor surrounding the central nozzle. Combustion mainly occurs in the center spout jet region and gasification mainly processes in the annular dense region [22,23]. In this process, spouting should be avoided. The spout-fluid bed coal gasifier should be operated in the flow pattern of “internal jet” or “jet in fluidized bed with bubbling”, had better in the flow pattern of “jet in fluidized bed with bubbling” [20]. Operation in this flow pattern can prolong the resident time of steam and air in the bed, making it uneasy for much steam and air to pass through the bed and wasted. This can enhance the gas and particle mixing between the spout region and the annular dense region [17], obtaining more uniform axial temperature profiles in order to improve the gasification efficiency. Thus, knowledge of flow characteristics at bed material larger than  $H_m$  is essentially important for special interest in applying the spout-fluid bed technology.

Refs. [14–20] sporadically treated of the flow behaviors when particles in bed larger than  $H_m$ . based on the previous and current studies, the flow behaviors under this condition can be grouped into some items as flows.

- (1) Stable and coherent spout or fountain is unable to be obtained. Periodic and incoherent spouting and spout-fluidizing can be observed at certain spouting and fluidizing gas flow rates [16,19,20]. However, in most cases, the spout is nonperiodic and incoherent with larger bubbles at the spout top. According to the definition of spout termination, this case is spout termination.
- (2) Relatively stable flow pattern of “jet in fluidized bed with slugging” can form. This flow pattern, as shown in Fig. 6, is very interesting for coal gasification. In this case, the spouting gas flow rate is generally less than minimum spouting gas flow rate. In practice, a pilot-scale 2MW<sub>t</sub> spout-fluid bed coal gasifier ( $D_t = 0.45$  m) in SEU of China has been successfully operated in the stable flow pattern of “jet in fluidized bed with slugging” at the initial bed height  $H_0 = 3.6$  m ( $H_0/D_t = 8$ , is over double of  $H_m$ , generally  $H_m/D_t$  is within 4.0) [22].
- (3) Compared to the case when the bed material is within the maximum spoutable bed height, the region of stable flow pattern is narrow. Flow instabilities will form at large gas flow rates especially large fluidizing gas flow rate, as shown in Fig. 7.

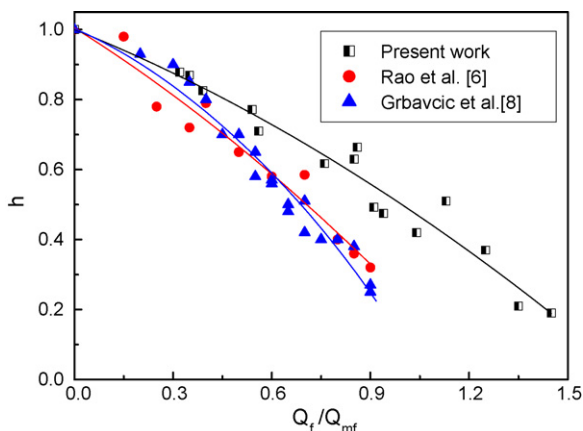


Fig. 5. Effect of fluidizing gas flow rate on the maximum spoutable bed height.

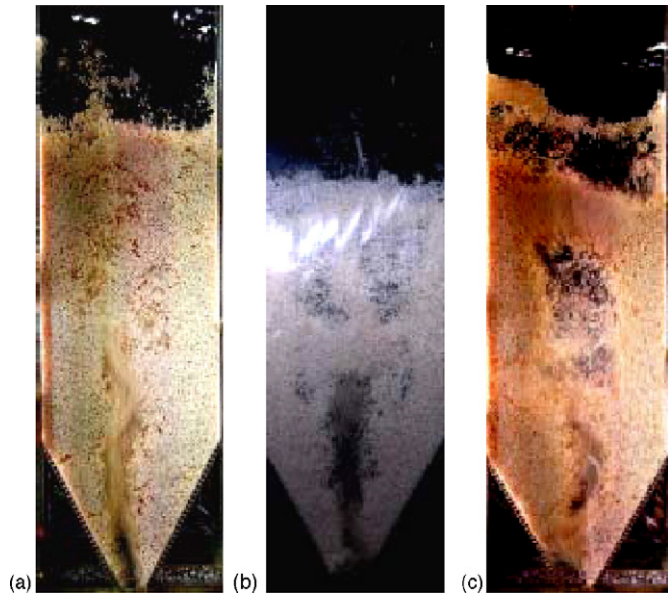


Fig. 6. Typical flow pattern images of jet in fluidized bed with bubbling (JFB): (a) polystyrene beads,  $H_0/D_t = 1.78$ ,  $D_i = 30$  mm,  $Q_i/Q_{mf} = 0.64$ ,  $Q_s/Q_{mf} = 3.20$ ; (b) polystyrene beads,  $H_0/D_t = 1.67$ ,  $D_i = 30$  mm,  $Q_i/Q_{mf} = 1.25$ ,  $Q_s/Q_{mf} = 2.80$ ; (c) polystyrene beads,  $H_0/D_t = 1.78$ ,  $D_i = 30$  mm,  $Q_i/Q_{mf} = 0.39$ ,  $Q_s/Q_{mf} = 3.20$ .

Summarily, when the particles in the bed larger than the maximum spoutable bed height is performed, the spout-fluid bed operated without a stable and coherent spout or fountain undoubtedly assembles the characteristics of jetting fluidized beds proposed in detail by Refs. [41–44].

The above discussion also implies that it is not absolutely right to think that the maximum spoutable bed height is directly related to the amount of materials that can be processed. Since spout-fluid beds can also be operated at the bed height larger than the maximum spoutable bed height for special interest such as gasification. However, knowledge of the maximum spoutable bed height and the flow behaviors when the bed material is larger

than the maximum spoutable bed height plays an important role in the design and application of spout-fluid beds.

### 3.4. Mechanism of spout termination

The mechanisms of spout termination in spouted beds have been reviewed and grouped into three different types when bed heights are larger than  $H_m$  by Mathur and Epstein [24]. They are: fluidization of the annular particles, choking of the spout and growth of instabilities at spout–annulus interface. The mechanism of spout termination in the spout-fluid bed has not been clarified so far. However, the following discussion might be helpful.

By analyzing of the flow pattern images recorded by digital CCD camera frame by frame, the mechanisms of spout termination in the spout-fluid bed is found to be slugging in the spout and growth of instabilities at the spout–annulus interface.

Choking of the spout is not the mechanism of spout termination due to the introduction of fluidizing gas into the bed, since the fluidizing gas would loosen the bed materials and benefit the spout jet to penetrate the bed [15,42,43]. However, on the other hand, the fluidizing gas easily dissipates the spouting gas momentum as the spout jet ascends in the bed, and large bubbles easily form in the upper region of the bed [43,45,46]. In this case, stable spouting is difficult to obtain even at large spouting gas flow rate. Instead, slugging caused by larger bubbles accompanied with growth of instabilities at spout–annulus interface caused by stochastic visible large bubbles in the boundary of spout jet and near the fluidizing gas distributor [20], as shown in Fig. 8.

Fluidization of the annular particles is also not the mechanism of spout termination in the spout-fluid bed. The particles in the annulus can be fluidized with introduction of fluidizing gas without reference to bed height. When the bed material is within the maximum spoutable bed height, relatively stable flow patterns of spouting and spout-fluidizing can be achieved. At the same

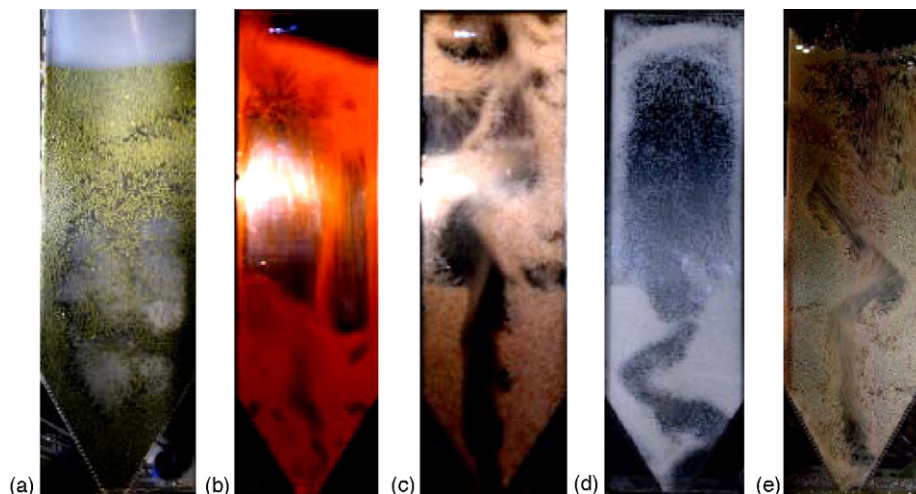


Fig. 7. Typical flow pattern images of spout termination: (a) mung beans,  $H_0/D_t = 1.67$ ,  $D_i = 20$  mm,  $Q_i/Q_{mf} = 2.20$ ,  $Q_s/Q_{mf} = 1.80$ ; (b) millet,  $H_0/D_t = 1.67$ ,  $D_i = 20$  mm,  $Q_i/Q_{mf} = 2.46$ ,  $Q_s/Q_{mf} = 2.0$ ; (c) polystyrene beads,  $H_0/D_t = 1.78$ ,  $D_i = 30$  mm,  $Q_i/Q_{mf} = 1.75$ ,  $Q_s/Q_{mf} = 3.60$ ; (d)  $H_0/D_t = 1.78$ ,  $D_i = 30$  mm,  $Q_i/Q_{mf} = 2.15$ ,  $Q_s/Q_{mf} = 4.0$ ; (e)  $H_0/D_t = 1.78$ ,  $D_i = 30$  mm,  $Q_i/Q_{mf} = 1.71$ ,  $Q_s/Q_{mf} = 3.20$ .

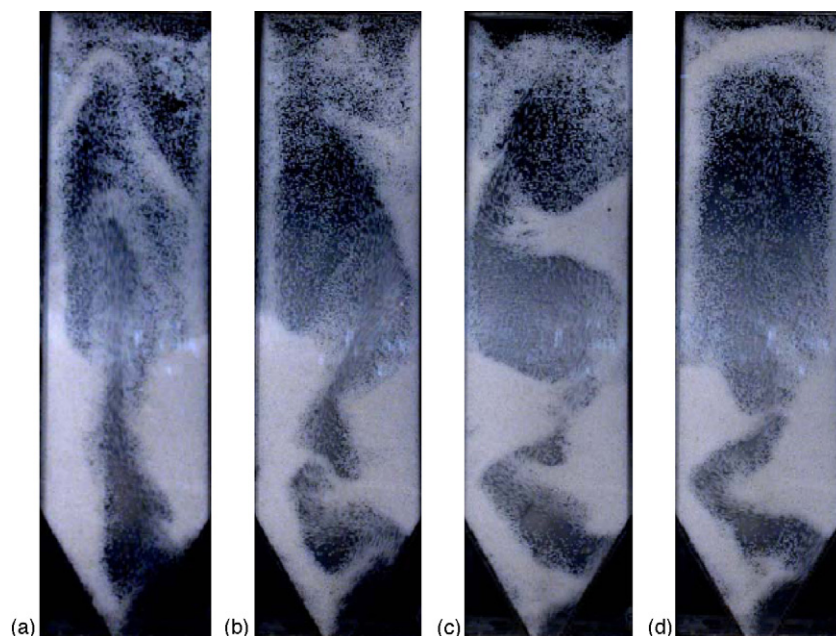


Fig. 8. Typical flow pattern images of spout termination recorded by CCD camera at  $\Delta t=0.125$  s: polystyrene beads,  $H_0/D_t=1.78$ ,  $D_t=30$  mm,  $Q_t/Q_{mf}=2.15$ ,  $Q_s/Q_{mf}=4.0$ .

time, the differential pressure signals show that particles in the annular region are fluidized. Though spout termination is found when the bed material is larger than the maximum spoutable bed height, it should not consider fluidization of the annular particles to be the mechanism of spout termination in the spout-fluid bed.

Thus, the present experiments consider that the mechanisms of spout termination in the spout-fluid bed should be slugging in the spout and growth of instabilities at the spout–annulus interface.

#### 4. Conclusions

Maximum spoutable bed heights  $H_m$  of a spout-fluid bed packed with six kinds of Geldart group D particles were studied. The effects of particle size, spout nozzle size and fluidizing gas flow rate on the maximum spoutable bed height were obtained. Besides, the flow characteristics when bed materials deeper than the maximum spoutable height were presented and the mechanisms of spout termination were discussed. The following conclusions were obtained.

- (1) The maximum spoutable bed height of spout-fluid bed decreases with increasing particle size and spout nozzle size, which appears the same trend to that of spouted beds.
- (2) The increasing of fluidizing gas flow rate leads to sharply decrease in the maximum spoutable bed height.
- (3) The existent correlations of the maximum spoutable bed height are observed to involve large discrepancies.
- (4) When bed materials larger than the maximum spoutable bed height are performed, the spout-fluid bed operated without a stable and coherent spout or fountain undoubtedly assembles the characteristics of jetting fluidized beds.

- (5) The maximum spoutable bed height is not directly related to the amount of materials that can be processed, since spout-fluid beds can also be operated at the bed height larger than the maximum spoutable bed height for special interest.
- (6) Slugging in the spout and growth of instabilities at the spout–annulus interface would cause the spout termination in spout-fluid bed.

#### Acknowledgements

Financial supports from the National Key Program of Basic Research in China (G199902210535, 2004CB217702, 2005CB221202 and 2006CB20030201), the National Natural Science Foundation of China (No. 50376010 and 20590367) and the Foundation of Graduate Creative Program of Jiangsu (XM04-28) were sincerely acknowledged.

#### References

- [1] C.J. Lim, A.P. Watkinson, G.K. Khoe, S. Low, N. Epstein, J.R. Grace, Spout, fluidized, spout-fluid bed combustion of bituminous coal, *Fuel* 67 (1988) 1211–1217.
- [2] D.L. Pianarosa, L.A.P. Freitas, C.J. Lim, J.R. Grace, O.M. Dogan, Voidage and velocity profiles in a spout-fluid bed, *Can. J. Chem. Eng.* 78 (2000) 132–142.
- [3] H. Littman, D.V. Vukovic, F.K. Zdanski, Z.B. Grbavcic, Pressure drop and flowrate characteristics of a liquid phase spout-fluid bed at the minimum spout-fluid flowrate, *Can. J. Chem. Eng.* 52 (1974) 174–179.
- [4] D.V. Vukovic, D.E. Hadzismajlovic, Z.B. Grbavcic, Flow regimes for spout fluidized beds, *Can. J. Chem. Eng.* 62 (1984) 825–829.
- [5] W. Sutanto, N. Epstein, J.R. Grace, Hydrodynamics of spout-fluid beds, *Powder Technol.* 44 (1985) 205–212.
- [6] K.B. Rao, A. Husain, C.D. Rao, Prediction of the maximum spoutable height in spout-fluid beds, *Can. J. Chem. Eng.* 63 (1985) 690–692.

- [7] J. Zhao, C.J. Lim, J.R. Grace, Flow regimes and combustion behavior in coal-burning spouted and spout-fluid beds, *Chem. Eng. Sci.* 42 (1987) 2865–2875.
- [8] Z.B. Grbavcic, D.V. Vukovic, D.E. Hadzismajlovic, R.V. Garic, H. Littman, Prediction of the maximum spoutable bed height in spout-fluid beds, *Can. J. Chem. Eng.* 69 (1991) 386–389.
- [9] B. Waldie, Separation and residence times of larger particles in a spout-fluid bed, *Can. J. Chem. Eng.* 70 (1992) 838–879.
- [10] M.Z. Anabtawi, B.Z. Uysal, R.Y. Jumah, Flow characteristics in a rectangular spout-fluid bed, *Powder Technol.* 169 (1992) 205–211.
- [11] Y.L. He, C.J. Lim, J.R. Grace, Spouted bed and spout-fluid bed behaviors in a column of diameter 0.91 m, *Can. J. Chem. Eng.* 70 (1992) 848–857.
- [12] B. Ye, C.J. Lim, J.R. Grace, Hydrodynamics of spouted and spout-fluidized beds at high temperature, *Can. J. Chem. Eng.* 70 (1992) 804–847.
- [13] R. Xiao, M. Zhang, B. Jin, X. Liu, Solids circulation flux and gas bypassing in a pressurized spout-fluid bed with a draft tube, *Can. J. Chem. Eng.* 80 (2002) 800–809.
- [14] W. Zhong, M. Zhang, Characterization of dynamic behavior of a spout-fluid bed with Shannon entropy analysis, *Powder Technol.* 159 (2005) 121–126.
- [15] W. Zhong, M. Zhang, Jet penetration depth in a two-dimensional spout-fluid bed, *Chem. Eng. Sci.* 60 (2005) 315–327.
- [16] W. Zhong, M. Zhang, Pressure fluctuation frequency characteristics in a spout-fluid bed by modern ARM power spectrum analysis, *Powder Technol.* 152 (2005) 52–61.
- [17] W. Zhong, M. Zhang, Experimental study of gas mixing in a spout-fluid bed, *AIChE J.* 52 (2006) 924–930.
- [18] W. Zhong, Y. Xiong, Z. Yuan, M. Zhang, DEM simulation of gas–solid flow behaviors in spout-fluid bed, *Chem. Eng. Sci.* 61 (2006) 157–1584.
- [19] W. Zhong, X. Chen, M. Zhang, Hydrodynamic characteristics of spout-fluid bed: pressure drop and minimum spouting/spout-fluidizing velocity, *Chem. Eng. J.* 118 (2006) 37–46.
- [20] W. Zhong, M. Zhang, B. Jin, X. Chen, Flow pattern and transition of rectangular spout-fluid bed, *Chem. Eng. Proc.* 45 (2006) 734–746.
- [21] J. Xiao, M. Zhang, Thermal performance analysis of pressurized partial gasification combined cycle (PPG-CC), in: *Proceedings of the Eighth SCEJ Symposium on Fluidization, Japan, 2002*, pp. 262–268.
- [22] R. Xiao, B. Jin, Y. Xiong, Y. Duan, Z. Zhong, X. Chen, Y. Huang, H. Zhou, M. Zhang, Coal gasification characteristics in a 2MWth second-generation PFB gasifier, in: *Proceedings of the 18th International Conference on Fluidized Bed Combustion, ASME, 2005*, pp. 185–192.
- [23] R. Xiao, M. Zhang, B. Jin, Y. Huang, H. Zhou, High-temperature air/steam-blown gasification of coal in a pressurized spout-fluid bed, *Energy Fuels* 20 (2006) 715–720.
- [24] K.B. Mathur, N. Epstein, *Spouted Beds*, Academic Press, New York, 1974.
- [25] H. Littman, M.H. Morgan, D.V. Vukovic, F.K. Zdanski, Z.B. Grbavcic, Theory for prediction the maximum spoutable height in a spouted bed, *Can. J. Chem. Eng.* 55 (1977) 497–501.
- [26] H. Littman, M.H. Morgan, D.V. Vukovic, F.K. Zdanski, Z.B. Grbavcic, Prediction of the maximum spoutable height and the average spout to inlet tube diameter ratio in spouted bed of spherical particles, *Can. J. Chem. Eng.* 57 (1979) 684–687.
- [27] G.S. McNab, J. Bridgwater, Solid mixing and segregation in spouted beds, *Proceedings of the Third European Conference on Mixing BHR Fluid Engineering (1979)* 125–140.
- [28] G.C. Rovero, M.H. Brereton, N. Epstein, J.R. Grace, L. Casalegno, N. Piccinini, Gas flow distribution in conical-base spouted beds, *Can. J. Chem. Eng.* 61 (1983) 289–296.
- [29] H. Littman, M.H. Morgan, New spouting regime in beds of coarse particles deeper than the maximum spoutable height, *Can. J. Chem. Eng.* 64 (1986) 505–508.
- [30] P.P. Chandnani, N. Epstein, in: V. Fluidization, K. Ostergaard, A. Sorensen (Eds.), *Spoutability and Spout Destabilization of Fine Particles with a Gas*, Engineering Foundation, New York, 1986, pp. 233–240.
- [31] A. Cecen, Maximum spoutable bed heights of fine particles spouted with air, *Can. J. Chem. Eng.* 72 (1994) 792–797.
- [32] M.L. Passos, A.S. Mujumdar, V.S.G. Raghavan, Prediction of the maximum spoutable bed height in two-dimensional spouted beds, *Powder Technol.* 74 (1993) 97–105.
- [33] M. Olazar, M.J. San, A.T. Aguayo, M. Arandes, J. Bilbao, *Design Factors of Conical Spouted Beds and Jet Spouted Beds*, vol. 32, *Industrial & Engineering Chemistry Research*, 1993, pp. 245–1250.
- [34] Y.L. He, C.J. Lim, J.R. Grace, Scale-up studies of spouted beds, *Chem. Eng. Sci.* 52 (1997) 329–339.
- [35] Y.L. He, C.J. Lim, J.R. Grace, Hydrodynamics of pressurized spouted beds, *Can. J. Chem. Eng.* 76 (1998) 696–701.
- [36] O.M. Dogan, L.A.P. Freitas, C.J. Lim, J.R. Grace, B. Luo, Hydrodynamics and stability of slot-rectangular spouted beds, *Chem. Eng. Commun.* 181 (2000) 225–242 (part I: thin bed).
- [37] L.A.P. Freitas, O.M. Dogan, C.J. Lim, J.R. Grace, B. Luo, Hydrodynamics and stability of slot-rectangular spouted beds, *Chem. Eng. Commun.* 181 (2000) 242–258 (part II: increasing bed thickness).
- [38] O.M. Dogan, B.Z. Uysal, J.R. Grace, Hydrodynamic studies in a half slot-rectangular spouted bed column, *Chem. Eng. Commun.* 191 (2004) 566–579.
- [39] Q. Zhu, C.J. Lim, N. Epstein, H.T. Bi, Hydrodynamic characteristics of a powder-particle spouted bed with powder entrained in spouting gas, *Can. J. Chem. Eng.* 83 (2005) 644–651.
- [40] M.S.J. Arnold, M.K. Laughlin, The British coal spout-fluid bed gasification process, *Can. J. Chem. Eng.* 70 (1992) 991–997.
- [41] W.C. Yang, D. Keairns, in: J.F. Davidson, D. Keairns (Eds.), *Design and Operating Parameters for a Fluidized Bed Agglomerating Combustor/Gasifier*, Fluidization I, Cambridge University Press, Cambridge, England, 1978, pp. 208–213.
- [42] W.C. Yang, Comparison of the jet phenomena in 30-cm and 3-m diameter semicircular fluidized beds, *Powder Technol.* 100 (1998) 147–160.
- [43] Q.J. Guo, G.X. Yue, J.Y. Zhang, Hydrodynamic behavior of a two-dimension jetting fluidized bed with binary mixtures, *Chem. Eng. Sci.* 56 (2001) 4685–4694.
- [44] Q.J. Guo, G.X. Yue, J.Y. Zhang, Flow Pattern Transition in a Large Jetting Fluidized Bed with a Vertical Nozzle, vol. 40, *Industrial and Engineering Chemistry Research*, 2001, pp. 3689–3696.
- [45] L.A. Behie, M.A. Bergougnou, C.G. Baker, W. Bulani, Jet momentum at a grid of large gas fluidized bed, *Can. J. Chem. Eng.* 48 (1970) 158–161.
- [46] L.A. Behie, M.A. Bergougnou, C.G. Baker, T.E. Base, Further studies on momentum dissipation of grid jets in a gas fluidized bed, *Can. J. Chem. Eng.* 49 (1971) 557–561.